

Experimental Investigations Of Axially Loaded Square Concrete-Filled Double Steel Tubular Slender Columns With Inner Circular Tube

Shicai Chen¹, Mizan Ahmed², Junchang Ci¹, Wensu Chen², Khaled Sennah³

¹ Department of Civil Engineering, Beijing University of Technology, Beijing, P.R. China

² School of Civil and Mechanical Engineering, Curtin University, Kent Street, Bentley, WA 6102, Australia

³ Department of Civil Engineering, Ryerson University, Toronto, Canada

chenshicai101@gmail.com; mizan.ahmed@curtin.edu.au; cjc_bjut@163.com; wensu.chen@curtin.edu.au; ksennah@ryerson.ca

Abstract – This paper reports an experimental work carried out on the square concrete-filled double steel tubular (CFDST) slender columns with an inner circular tube under concentric loading. The influences of the column slenderness ratio and the thickness of the inner steel tube on the performance of the square CFDST slender column are investigated. The applicability of the design recommendations given by Eurocode 4 for conventional concrete-filled steel tubular columns is evaluated in designing square CFDST slender columns under concentric loading. It is found that the performance of the square CFDST slender column is significantly influenced by the column slenderness ratio and the thickness of the inner steel tube. Furthermore, the design specification given by Eurocode 4 significantly underestimates the ultimate strength of square CFDST slender columns under concentric loading.

Keywords: Concrete-filled steel tubes; concentric loading; slender columns; composite columns.

1. Introduction

The composite action between the steel and concrete results in the improvement of the strength, ductility, fire and seismic performance of concrete-filled steel tubular (CFST) columns compared to reinforced concrete columns. The confinement effect on a circular CFST column is more uniform than that of a square or rectangular cross-section of a CFST column, thus the performance of a circular CFST column is much superior to that of its square or rectangular counterparts [1]. Furthermore, the steel tube of a square or rectangular CFST column is more susceptible to the local buckling than that of a circular tube, which significantly influences its structural performance [2]. However, the simplicity of connecting a square or rectangular CFST column to the adjacent beam makes it a preferred cross-section compared to a circular CFST column [3, 4]. Significant research studies were performed to improve the cross-section of CFST columns that provides better bearing capacity and offers simplicity in connecting to adjacent beams such as investigating the cross-section of CFST columns including octagonal shape [5-8], hexagonal shape [9-13], round-ended [14-17] and elliptical shape [18-22].

Recently, square concrete-filled double steel tubular (CFDST) column with an inner circular tube, as illustrated in Fig. 1 has been proposed as an innovative cross-section of CFST columns that offers the advantages of both the square and circular CFST columns [4, 23]. To study their structural performance, researchers performed tests on square CFDST columns under different loading conditions [24-28]. However, most of the tests were carried out on short CFDST columns, where the length-to-outer width ratio (L/B_o) was limited to 4 to prevent the global buckling from occurring [29-32]. Test on CFDST slender columns was only reported by Xiong et al. [30], where the concrete compressive strength was about 180 MPa. It was found that for slender columns, the effectiveness of using ultra-high-strength concrete is very minimal. Ahmed et al. [33, 34] developed numerical models in investigating the performance of eccentrically loaded CFDST slender columns with and without preload effects. Design models to predict the ultimate strength of CFDST slender columns were proposed based on numerical modeling.

This study reports a series of tests carried out on square CFDST slender columns under concentric loading. The test parameter includes the column slenderness ratio and the thickness of the inner steel tube. The accuracy of the design specifications given by Eurocode 4 [35] for conventional CFST columns is evaluated in predicting the ultimate strength of CFDST slender columns under concentric loading.

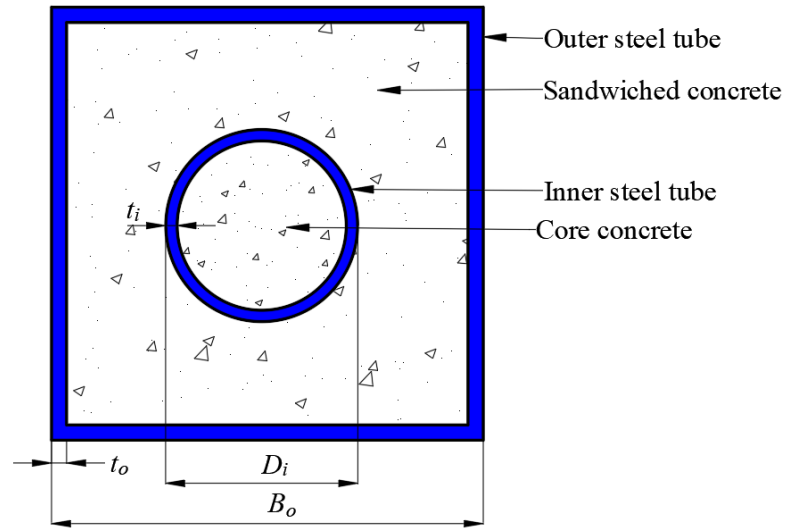


Fig. 1: Cross-section of a square CFDST column with an inner circular tube. (where B_o and D_i are the width of the outer tube and diameter of the inner tube, respectively; t_o and t_i are the thickness of the outer and inner steel tube, respectively).

2. Experiments on square CFDST slender columns

2.1. Test specimens

Eight square CFDST columns were tested under concentric loading including two short columns, where L/B_o ratio of the columns was 4. The cross-section of the outer square tube ($B_o \times t_o$) was identical to 200×4.5 mm for all the tested columns. The diameter of the inner circular steel tube was 114 mm for all tested columns with two different thicknesses of the steel tubes of 2.5 mm and 3.5 mm, which were used to study the influences of the thickness of the inner steel tube on the performance of CFDST slender columns. The tested columns were divided into two groups (Group 1 and Group 2) according to their thickness. Different slenderness ratios of the columns were investigated for each Group. For columns in Group 1, the L/B_o ratio of the column varied from 4, 6, 8, 10 and 12; whereas for columns in Group 2, the L/B_o ratio of the column varied from 4, 8 and 12. Table 1 summarizes the details of the test columns.

In making CFDST columns, the outer and inner steel tubes were placed concentrically and welded with two steel bars. Readily available steel hollow tubes having a nominal yield strength of 235 MPa were used to construct CFDST columns. The hollow steel tubes were then filled with concrete having the same compressive strength.

2.2 Material properties

Three tensile coupon tests were performed according to GB/T 228.1-2010 [36] to obtain the material properties of steel tubes. The yield stress of the steel tubes having a thickness of 2.5, 3.5 and 4.5 mm was measured as 314, 329 and 357 MPa, respectively. The tensile stress of the steel tubes having a thickness of 2.5, 3.5 and 4.5 mm was measured as 375, 415 and 482 MPa, respectively. The elastic modulus of the steel tubes having a thickness of 2.5, 3.5 and 4.5 mm was calculated as 198, 205 and 203 GPa, respectively. Three concrete cubes ($150 \text{ mm} \times 150 \text{ mm} \times 150 \text{ mm}$) were cast to measure the compressive strength of the concrete. The cubes were cast at the same time as the tested columns and cured under the same condition. From the compression tests performed after 28 days of casting, the average compressive cube strength was measured as 47 MPa.

Table 1: Details of test specimens.

Group	Specimen	Outer tube	Inner tube	L	L/B_o	f'	N_{exp}	N_{cal}	$\frac{N_{cal}}{N_{exp}}$
-------	----------	------------	------------	-----	---------	------	-----------	-----------	---------------------------

		B_o (mm)	t_o (mm)	D_i (mm)	t_i (mm)	(mm)		(MPa)	(kN)	(kN)	
Group 1	S-1-4	200	4.5	114	3.5	800	4	47	3265	2690	0.82
	S-1-6	200	4.5	114	3.5	1200	6	47	3211	2620	0.82
	S-1-8	200	4.5	114	3.5	1600	8	47	3186	2505	0.79
	S-1-10	200	4.5	114	3.5	2000	10	47	3172	2387	0.75
	S-1-12	200	4.5	114	3.5	2400	12	47	2978	2264	0.76
Group 2	S-2-4	200	4.5	114	2.5	800	4	47	3102	2535	0.82
	S-2-8	200	4.5	114	2.5	1600	8	47	2957	2366	0.80
	S-2-12	200	4.5	114	2.5	2400	12	47	2876	2142	0.74
Mean											0.79
Standard Deviation (SD)											0.03
Coefficient of Variance (CoV)											0.04

2.3. Experimental setup

The experimental program was carried out at the Beijing University of Technology, China using a 4000 kN hydraulic testing machine. For safety purposes, all specimens were tested horizontally due to the height of the longest test specimens exceeded the height of the reaction frame. To eliminate the elephant foot buckling like premature failure mode, both ends of all the specimens were clamped with steel clamps. Two sets of loading devices comprised of loading and adapter plates were used to apply load in the tested columns. The end faces of the specimens were coated with superhard gypsum prior to loading the column in the testing frame to ensure the evenness and to eliminate any gap between the column and loading plates. The test setup of a typical specimen is shown in Fig. 2.

The distributions of the strain of the tested columns were measured both at the compression and tension sides of the tested columns at midspan using bi-directional strain gauges attached to the outer tube. Both axial and lateral displacement of the tested columns were measured using displacement sensors. Except for columns S-1-12 and S-2-12, the lateral displacement of the test columns was measured using three displacement sensors. For columns S-1-12 and S-2-12, five displacement sensors were used to measure the lateral displacement. Two displacement sensors were used to record the axial displacements of the columns. The tested columns were preloaded to 100 kN to remove any possible gap between the specimens and the loading devices prior to recording the data. The columns were tested under displacement control at the rate of 1 mm/min. The test stopped when the axial displacement of the specimens reached 30 mm. The DH18 data acquisition system was employed to collect data for applied load, strain gauges and displacement sensors.

3. Experimental results

The typical failure modes of the tested slender columns were local buckling of the outer steel tube and global buckling of the columns. Figure 3 illustrates the typical modes of failure of the tested columns. Utilization of the steel clamps at the column ends was found to successfully prevent the failure modes of elephant foot buckling under axial loading. From Table 1, it can be seen that increasing the L/B_o ratio of the column significantly reduced the ultimate strength of CFDST columns. The ultimate compressive strength of the columns in Group 1 decreased by 8.8% when the L/B_o ratio of the column increased from 4 to 12. For columns in Group 2, the ultimate compressive strength of the columns decreased by 7.3% for the increase of the L/B_o ratio of the column from 4 to 12. Furthermore, decreasing the inner steel tube thickness decreased the ultimate compressive strength of the columns. The ultimate compressive strength of the columns S-2-4 and S-2-8 was 5% and 7.2% lower than the ultimate compressive strength of the columns S-1-4 and S-1-8, respectively.



Fig. 2: Typical test setup of square CFDST slender column under concentric loading.



Fig. 3: Typical failure mode of square CFDST slender columns under concentric loading.

The axial load-midspan displacement curves of the tested specimens are presented in Fig. 4. Generally, the descending portion of the axial load-midspan lateral displacement curves of the tested columns can be seen as more flat as the column reached the ultimate compressive strength; however, the rapid decrease in the midspan displacement for columns S-1-6 and S-2-8 can be due to the excessive local buckling of the steel tube.

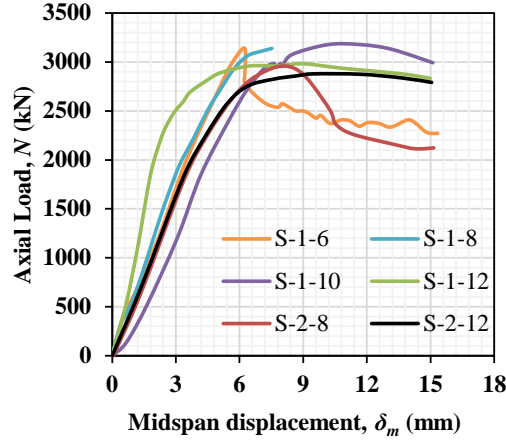


Fig. 4: Axial load-midspan lateral displacement curves of square CFDST slender columns.

4. Design model

This section evaluates the applicability of existing design specifications specified by Eurocode 4 [35] for conventional CFST columns in predicting the ultimate compressive strength of square CFDST slender columns. Eurocode 4 only considers confinement effects for the circular section. Based on Eurocode 4, the ultimate compressive strength of square CFDST short columns (N_u) with an inner circular tube can be calculated as:

$$N_u = A_{soe} f_{sy0} + A_{co} f'_{co} + \eta_a A_{si} f_{syi} + A_{ci} f'_{ci} \left(1 + \eta_c \frac{t_i}{D_i} \frac{f_{syi}}{f'_{ci}}\right) \quad (1)$$

in which A_{soe} , A_{si} , A_{co} and A_{ci} are the cross-sectional area of the outer tube, inner tube, sandwiched concrete and core concrete, respectively; D_i is the diameter of the inner tube; t_i is the thickness of the inner tube; f_{sy0} and f_{syi} are the yield stress of the outer and inner tube, respectively; f'_{co} and f'_{ci} are the concrete cylindrical compressive strength of sandwiched and core concrete, respectively. As in this study, the compressive strength of concrete was measured using compression tests of concrete cube, the concrete cube strength was converted to cylindrical strength using a factor of 0.85 proposed by Oehlers and Bradford [37]. In Eq. (1) parameters η_a and η_c are calculated as

$$\eta_a = 0.25 (3 + 2\bar{\lambda}) \quad (\eta_a \leq 1.0) \quad (2)$$

$$\eta_c = 4.9 - 18.5 \bar{\lambda} + 17 \bar{\lambda}^2 \quad (\eta_c > 0) \quad (3)$$

in which $\bar{\lambda}$ is the relative slenderness ratio of the column expressed as:

$$\bar{\lambda} = \sqrt{\frac{N_u}{N_{cr}}} \quad (4)$$

in which N_{cr} is the Euler buckling calculated as:

$$N_{cr} = \frac{\pi^2 (EI)_{eff}}{L^2} \quad (5)$$

in which $(EI)_{eff}$ is the effective flexural stiffness calculated as:

$$(EI)_{eff} = E_{s,so} I_{s,so} + 0.6 E_{cm,co} I_{c,co} + E_{s,si} I_{s,si} + 0.6 E_{cm,ci} I_{c,ci} \quad (6)$$

$$E_{cm} = 22000 \left(\frac{f'_c + 8}{10} \right)^{1/3} \quad (7)$$

in which $E_{s,so}$ and $E_{s,si}$ are the elastic modulus of outer and inner steel tube, respectively; $E_{cm,co}$ and $E_{cm,ci}$ are the elastic modulus of sandwiched and core concrete, respectively; $I_{s,so}$ and $I_{s,si}$ are the second moment of area of the outer and inner steel tube, respectively; $I_{c,co}$ and $I_{c,ci}$ are the second moment of area of the sandwiched and core concrete, respectively.

Eurocode 4 specified a slenderness limit $\frac{B_o}{t_o} \leq 52 \sqrt{\frac{235}{f_{syo}}}$ for steel tube beyond which local buckling should be considered.

As the tested columns in this study exceed the limit specified by Eurocode 4, the effective width of the outer tube was calculated using the formula suggested by Eurocode 4 and Gardner and Theofanous [38] as:

$$\rho = \frac{0.772}{\bar{\lambda}_p} - \frac{0.079}{\bar{\lambda}_p^2} \quad (8)$$

$$\bar{\lambda}_p = \sqrt{\frac{12(1-\nu_s^2)f_{syo}}{k\pi E_{so}}} \frac{B_o}{t_o} \quad (9)$$

in which ρ is the local buckling reduction factor; $\bar{\lambda}_p$ is the plate slenderness; E_{so} is the elastic modulus of outer steel tube; k is the buckling coefficient, taken as 4 and ν_s is Poisson's ratio of steel tube, taken as 0.3.

Eurocode 4 suggested a slenderness reduction factor χ to consider the slenderness ratio in calculating the ultimate compressive strength of slender section written as:

$$N_{u,EC4} = \chi N_u \quad (10)$$

in which χ is suggested in Eurocode 3 [39] as:

$$\chi = \frac{1}{\varphi + \sqrt{\varphi^2 - \bar{\lambda}^2}} \leq 1.0 \quad (11)$$

$$\varphi = \frac{1 + \alpha(\bar{\lambda} - 0.2) + \bar{\lambda}^2}{2} \quad (12)$$

in which α is the imperfection factor corresponding to the relevant buckling curve taken as 0.49 based on buckling curve 'c' for CFDST columns.

Based on the comparisons of the experimental and predicted ultimate compressive strength of CFDST columns given in Table 1, it can be seen that Eurocode 4 significantly underestimates the ultimate compressive strength of CFDST columns under concentric loading. The mean ratio of the predicted-to-experimental ultimate compressive strength (N_{cal} / N_{exp}) was calculated as 0.79 with a standard deviation of 0.03.

5. Conclusion

This paper investigates the mechanical performance of square CFDST slender column under concentric loading. Test results on eight CFDST columns including 2 short columns are presented. Test results show that the ultimate compressive strength of square CFDST slender columns is influenced by the L/B_0 ratio of the column and the thickness of the inner steel tube. Increasing the L/B_0 ratio of the column or decreasing the thickness of the inner steel tube reduces the ultimate compressive strength of the columns under concentric loading. Based on the comparisons of the predicted ultimate strength of CFDST columns using the design specifications of conventional CFST columns

specified by Eurocode 4, it is found that Eurocode 4 significantly underestimates the ultimate strength of CFDST slender columns under concentric loading.

References

- [1] Sakino K, Nakahara H, Morino S, and Nishiyama I. Behavior of centrally loaded concrete-filled steel-tube short columns. *Journal of Structural Engineering* 2004;130(2):180-188.
- [2] Liang QQ, Uy B, and Liew JYR. Local buckling of steel plates in concrete-filled thin-walled steel tubular beam-columns. *Journal of Constructional Steel Research* 2007;63(3):396-405.
- [3] Wang ZB, Tao Z, and Yu Q. Axial compressive behaviour of concrete-filled double-tube stub columns with stiffeners. *Thin-Walled Structures* 2017;120:91-104.
- [4] Ahmed M, Liang QQ, Patel VI, and Hadi MNS. Nonlinear analysis of rectangular concrete-filled double steel tubular short columns incorporating local buckling. *Engineering Structures* 2018;175:13-26.
- [5] Ding F-X, Li Z, Cheng S, and Yu Z-W. Composite action of octagonal concrete-filled steel tubular stub columns under axial loading. *Thin-Walled Structures* 2016;107:453-461.
- [6] Hassanein MF, Patel VI, Elchalakani M, and Thai H-T. Finite element analysis of large diameter high strength octagonal CFST short columns. *Thin-Walled Structures* 2018;123:467-482.
- [7] Zhu J-Y and Chan T-M. Experimental investigation on octagonal concrete filled steel stub columns under uniaxial compression. *Journal of constructional steel research* 2018;147:457-467.
- [8] Ahmed M and Liang QQ. Numerical modeling of octagonal concrete-filled steel tubular short columns accounting for confinement effects. *Engineering Structures* 2020;226:111405.
- [9] Ding F-X, Li Z, Cheng S, and Yu Z-W. Composite action of hexagonal concrete-filled steel tubular stub columns under axial loading. *Thin-Walled Structures* 2016;107:502-513.
- [10] Xu W, Han L-H, and Li W. Performance of hexagonal CFST members under axial compression and bending. *Journal of Constructional Steel Research* 2016;123:162-175.
- [11] Hassanein MF, Patel VI, and Bock M. Behaviour and design of hexagonal concrete-filled steel tubular short columns under axial compression. *Engineering Structures* 2017;153:732-748.
- [12] Liu J, Li Z, and Ding F-X. Experimental Investigation on the Axially Loaded Performance of Notched Hexagonal Concrete-Filled Steel Tube (CFST) Column. *Advances in Civil Engineering* 2019;2019:2612536.
- [13] Ahmed M and Liang QQ. Numerical analysis of concentrically loaded hexagonal concrete-filled steel tubular short columns incorporating concrete confinement. *Advances in Structural Engineering* 2021;13694332211004111.
- [14] Wang Z, Chen J, Xie E, and Lin S. Behavior of concrete-filled round-ended steel tubular stub columns under axial compression. *Journal of Building Structures* 2014;35(7):123-130 (Chinese).
- [15] Hassanein MF and Patel VI. Round-ended rectangular concrete-filled steel tubular short columns: FE investigation under axial compression. *Journal of Constructional Steel Research* 2018;140:222-236.
- [16] Piquer A, Ibañez C, and Hernández-Figueirido D. Structural response of concrete-filled round-ended stub columns subjected to eccentric loads. *Engineering Structures* 2019;184:318-328.
- [17] Ahmed M and Liang QQ. Numerical analysis of thin-walled round-ended concrete-filled steel tubular short columns including local buckling effects. *Structures* 2020;28:181-196.
- [18] Ahmed M, Ci J, Yan X-F, and Chen S. Nonlinear analysis of elliptical concrete-filled stainless steel tubular short columns under axial compression. *Structures* 2021;32:1374-1385.
- [19] Ahmed M and Liang QQ. Computational simulation of elliptical concrete-filled steel tubular short columns including new confinement model. *Journal of Constructional Steel Research* 2020;174:106294.
- [20] Cai Y, Quach W-M, and Young B. Experimental and numerical investigation of concrete-filled hot-finished and cold-formed steel elliptical tubular stub columns. *Thin-Walled Structures* 2019;145:106437.
- [21] Hassanein MF, Patel VI, El Hadidy AM, Al Abadi H, and Elchalakani M. Structural behaviour and design of elliptical high-strength concrete-filled steel tubular short compression members. *Engineering Structures* 2018;173:495-511.
- [22] Lam D, Gardner L, and Burdett M. Behaviour of axially loaded concrete filled stainless steel elliptical stub columns. *Advances in Structural Engineering* 2010;13(3):493-500.
- [23] Ci J, Chen S, Jia H, Yan W, Song T, and Kim K-S. Axial compression performance analysis and bearing capacity calculation on square concrete-filled double-tube short columns. *Marine Structures* 2020;72:102775.

- [24] Pei WJ, Research on mechanical performance of multibarrel tube-confined concrete columns. 2005, Chang'an University, Xian, China, ME Thesis
- [25] Qian J, Zhang Y, Ji X, and Cao W. Test and analysis of axial compressive behavior of short composite-sectioned high strength concrete filled steel tubular columns. *Journal of Building Structures* 2011;32(12):162-169 (in Chinese).
- [26] Qian J, Zhang Y, and Zhang W. Eccentric compressive behavior of high strength concrete filled double-tube short columns. *Journal of Tsinghua University (Science and Technology)* 2015;55(1):1-7 (in Chinese).
- [27] Xiong MX, Xiong DX, and Liew JYR. Behaviour of steel tubular members infilled with ultra high strength concrete. *Journal of Constructional Steel Research* 2017;138:168-183.
- [28] Ahmed M, Liang QQ, Patel VI, and Hadi MNS. Experimental and numerical studies of square concrete-filled double steel tubular short columns under eccentric loading. *Engineering Structures* 2019;197:109419.
- [29] Ahmed M, Liang QQ, Patel VI, and Hadi MNS. Behavior of eccentrically loaded double circular steel tubular short columns filled with concrete. *Engineering Structures* 2019;201:109790.
- [30] Xiong MX, Xiong DX, and Liew JYR. Axial performance of short concrete filled steel tubes with high-and ultra-high-strength materials. *Engineering Structures* 2017;136:494-510.
- [31] Ci J, Ahmed M, Tran V-L, Jia H, and Chen S. Axial compressive behavior of circular concrete-filled double steel tubular short columns. *Advances in Structural Engineering* 2021:13694332211046345.
- [32] Wan CY and Zha XX. Nonlinear analysis and design of concrete-filled dual steel tubular columns under axial loading. *Steel and Composite Structures* 2016;20(3):571-597.
- [33] Ahmed M, Liang QQ, Patel VI, and Hadi MNS. Local-global interaction buckling of square high-strength concrete-filled double steel tubular slender beam-columns. *Thin-Walled Structures* 2019;143:106244.
- [34] Ahmed M, Liang QQ, Patel VI, and Hadi MNS. Nonlinear analysis of square concrete-filled double steel tubular slender columns incorporating preload effects. *Engineering Structures* 2020;207:110272.
- [35] Eurocode 4: Design of Composite Steel and Concrete Structures-Part 1-1: General Rules and Rules for Buildings. European Committee for Standardization (CEN) Brussels, Belgium. 2004.
- [36] GB/T 228.1-2010. Metallic materials-Tensile testing-Part 1:Method of test at room temperature. China. 2010.
- [37] Oehlers DJ and Bradford MA, *Elementary behaviour of composite steel and concrete structural members*. Oxford U.K.: Butterworth-Heinemann, 1999.
- [38] Gardner L and Theofanous M. Discrete and continuous treatment of local buckling in stainless steel elements. *Journal of Constructional Steel Research* 2008;64(11):1207-1216.
- [39] Eurocode 3: Design of Steel Structures-Part 1-1: General Rules and Rules for Buildings. European Committee for Standardization (CEN) Brussels, Belgium. 2005.